

This article was downloaded by:[Texas A & M University]
[Texas A & M University]

On: 30 January 2007

Access Details: [subscription number 762304754]

Publisher: Taylor & Francis

Informa Ltd Registered in England and Wales Registered Number: 1072954

Registered office: Mortimer House, 37-41 Mortimer Street, London W1T 3JH, UK



Journal of Modern Optics

Publication details, including instructions for authors and subscription information:

<http://www.informaworld.com/smpp/title-content=t713191304>

Semiquantitative model for response of biological molecules containing C, N, O and H to laser pulses, with initial application to dipicolinic acid

Petra Sauer^a; Roland E. Allen^a

^a Institute for Quantum Studies and Physics Department, Texas A&M University, College Station, TX 77843, USA

To link to this article: DOI: 10.1080/09500340600898247

URL: <http://dx.doi.org/10.1080/09500340600898247>

Full terms and conditions of use: <http://www.informaworld.com/terms-and-conditions-of-access.pdf>

This article maybe used for research, teaching and private study purposes. Any substantial or systematic reproduction, re-distribution, re-selling, loan or sub-licensing, systematic supply or distribution in any form to anyone is expressly forbidden.

The publisher does not give any warranty express or implied or make any representation that the contents will be complete or accurate or up to date. The accuracy of any instructions, formulae and drug doses should be independently verified with primary sources. The publisher shall not be liable for any loss, actions, claims, proceedings, demand or costs or damages whatsoever or howsoever caused arising directly or indirectly in connection with or arising out of the use of this material.

© Taylor and Francis 2007

Semiquantitative model for response of biological molecules containing C, N, O and H to laser pulses, with initial application to dipicolinic acid

PETRA SAUER and ROLAND E. ALLEN*

Institute for Quantum Studies and Physics Department,
Texas A&M University, College Station, TX 77843, USA

(Received 20 April 2006; in final form 19 June 2006)

We have constructed a semiquantitative model which can be used to treat the response of molecules containing carbon, nitrogen, oxygen and hydrogen to ultrafast laser pulses. The parameters for the pairwise interaction of both nitrogen and oxygen are obtained from a simple scaling of carbon and hydrogen parameters calculated by Frauenheim and co-workers. For the initial application of this model, we have chosen dipicolinic acid (DPA), an important constituent of biological spores. The equilibrium bond lengths of all of the test molecules, including DPA, are within 5% of the experimental bond lengths. The calculated molecular orbital structure of DPA near the HOMO–LUMO gap region shows three nearly degenerate occupied molecular orbitals and two nearly degenerate unoccupied orbitals. Photoexcitation with an ultrashort 5 fs FWHM laser pulse matched to the HOMO–LUMO gap energy produced transitions from the lowest of the three nearly degenerate occupied orbitals to both of the nearly degenerate unoccupied molecular orbitals. The precise nature of the transition depends on the polarization of the laser pulse. These results are shown to be in qualitative agreement with fully *ab initio* methods.

1. Introduction

The interaction of ultrafast laser pulses with chemical and biological molecules can lead to a wide variety of molecular processes including bond breakage and formation, molecular isomerization, and the excitation of specific vibrational frequencies [1]. Since these processes happen on a femtosecond time scale, there is a need for realistic excited state simulations that can add insight and a fuller understanding to experimental studies. One common approach, used in many fully *ab initio* methods, is to artificially promote an electron to an excited state energy level. Although this approach can provide accurate information, it cannot describe the effect of variation in the laser pulse parameters on the outcome of the simulation.

*Corresponding author. Email: allen@physics.tamu.edu

These effects can only be included if both the electronic and nuclear configuration are calculated as a function of time. As this type of molecular dynamics simulation requires a time step on the order of attoseconds, the integration of a fully *ab initio* method into a molecular dynamics simulation becomes computationally prohibitive for many interesting chemical and biological systems. We therefore use a semi-empirical scheme in which the electronic and nuclear properties are parameterized from density functional theory. Although some of the accuracy of the fully *ab initio* methods is sacrificed, this method allows us to simulate molecules containing hundreds of atoms on femtosecond timescales with attosecond time steps.

We use the semi-empirical radiation-ion-dynamics (SERID) technique that is described in detail elsewhere [2]. Briefly, this method treats the valence electrons quantum mechanically and both the motion of the ion cores and the radiation field classically. The electronic wavefunctions are constructed by solving the time-dependent Schrödinger equation in a non-orthogonal basis at every time step:

$$i\hbar \frac{\partial \psi_j}{\partial t} = \mathbf{S}^{-1} \mathbf{H} \psi_j,$$

where \mathbf{S} is the overlap matrix for the atomic orbitals. The laser excitation is included as a perturbation to the Hamiltonian via a Peierls substitution. The Hamiltonian matrix, overlap matrix and ion-ion repulsive potential are determined from density-functional calculations. Parameters for the pairwise interaction of carbon-carbon (C-C), carbon-hydrogen (C-H) and hydrogen-hydrogen (H-H) were calculated by Frauenheim and co-workers [3].

2. SERID parameters for nitrogen and oxygen containing molecules

This group has used the Frauenheim parameters to successfully simulate the dynamics of a variety of organic molecules including stilbene [4], butadiene [2], benzene [5] and fullerenes [6]. In order to study a larger array of compounds, we have developed a simple scheme that scales the original density functional based parameters for carbon and hydrogen to include pairwise interactions with nitrogen and oxygen. In the future we would like to extend this scheme to include other row atoms as well. The tight-binding Hamiltonian matrix elements are scaled to reproduce the electronic properties of the new interaction and the repulsive potential is scaled to match the atomic equilibrium properties (i.e. bond lengths and vibrational frequencies) of the diatomic molecule corresponding to the desired interaction.

In order to fit to the electronic properties of the new interaction, we first scaled the on-diagonal Hamiltonian matrix elements, H_{ii} , to the orbital s and p energies taken from a Hartree-Fock (HF) calculation [7] of the new atom. Since the original H_{ii} values are not identical to the HF calculated atomic energies, we have scaled the new matrix elements by the ratio of the two values (see table 1). The off-diagonal elements, H_{ij} , were then scaled so that the energy eigenvalue difference between two appropriately chosen orbitals, called the active space region, matches the same

Table 1. Hartree–Fock atomic orbital energies with minus sign omitted (units are au). These values are scaled to the original Frauenheim values [3] of 0.2386 au for the 1s state of hydrogen and 0.5049 au and 0.1944 au for the 2s and 2p states of carbon.

	H	C	N	O
1s	0.5000	–	–	–
2s	–	0.7121	0.9637	1.2504
2p	–	0.4069	0.5087	0.6162

Table 2. Description of the active space (AS) orbitals used for the scaling of each pairwise interaction and the corresponding scale factor, η . Only the valence orbitals are considered.

Molecule	AS	ΔE_{AS} (eV)	η
N ₂	2–7	14.31	1.38
CN	2–7	11.94	1.13
O ₂	2–8	22.62	0.67
CO	2–7	14.86	1.38
NO	2–8	19.16	0.62
NH	2–5	10.07	0.81
OH	2–5	12.32	0.94

energy eigenvalue difference from a DFT calculation performed using the B3LYP functional and Dunning’s correlation consistent basis sets [8].

Table 2 shows the active space used, the eigenvalue difference and the scale factor obtained for each atom pair. All non-hydrogen containing molecules were scaled from the original carbon–carbon interaction and the hydrogen containing molecules were scaled from the carbon–hydrogen interactions. Since the matrix elements are defined for each value of r , we have also scaled the value of r by a constant:

$$r' = \frac{r}{\beta},$$

where we defined β to be the ratio of the old equilibrium bond length to the new equilibrium bond length.

Once the Hamiltonian matrix elements are fit to the electronic properties of the new interaction, the coefficients of the nuclear repulsion are scaled to match the equilibrium bond lengths and vibrational frequencies of the corresponding diatomic molecule. The original form for effective nuclear repulsion as given by Frauenheim and co-workers [3] is

$$V(R) = \sum_{n=2}^9 a_n R^n,$$

$$R = r_c - r,$$

where the values of the coefficients, a_n , and the cut-off value for the potential, r_c , are determined through a fit to density functional values. In order to refit these values to the equilibrium properties of the new diatomic molecule we have scaled this potential in the following manner

$$V'(R') = (c_0 + c_1 R')V(R),$$

where the values of the constants, c_0 and c_1 , are determined from the equilibrium conditions:

$$\begin{aligned} \left(\frac{dE_{\text{rep}}}{dr} + \frac{dE_{\text{elec}}}{dr} \right)_{r=r_0} &= 0, \\ \left(\frac{d^2 E_{\text{rep}}}{dr^2} + \frac{d^2 E_{\text{elec}}}{dr^2} \right)_{r=r_0} &= M\omega^2. \end{aligned}$$

These equilibrium conditions depend on the first and second derivatives of the electronic contributions to the energy of the system. These derivatives were evaluated numerically at the equilibrium bond length from the scaled Hamiltonian and overlap matrix elements according to

$$\begin{aligned} \frac{\partial E_{\text{elec}}}{\partial x} &= \sum_n \Psi_n^\dagger \left(\frac{\partial H}{\partial x} - \varepsilon_n \frac{\partial S}{\partial x} \right) \Psi_n f(n), \\ \frac{\partial^2 E_{\text{elec}}}{\partial x^2} &= 2 \sum_n \sum_{m \neq n, \varepsilon_m \neq \varepsilon_n} \frac{|\Psi_n^\dagger (\frac{\partial H}{\partial x} - \varepsilon_n \frac{\partial S}{\partial x}) \Psi_m|^2}{\varepsilon_n - \varepsilon_m} f(n) \\ &\quad + 2 \sum_n \Psi_n^\dagger \left(\frac{\partial^2 H}{\partial x^2} - 2 \frac{\partial \varepsilon_n}{\partial x} \frac{\partial S}{\partial x} - \varepsilon_n \frac{\partial^2 S}{\partial x^2} \right) \Psi_n f(n). \end{aligned}$$

This scaling scheme was chosen in order to adjust the equilibrium properties to the desired values without drastically altering the shape of the effective nuclear repulsion curve.

This method of scaling presents a discrepancy in the energetic ordering of the orbitals for the O_2 molecule. The ground state electronic configuration of the 8 valence electrons of the C_2 molecule is $(1\sigma_g)^2(1\sigma_u)^2(\pi_u)^2(\pi_u)^2$. The unoccupied molecular orbitals are $2\sigma_g, \pi_g, \pi_g$ and $2\sigma_u$, ordered from lowest to highest. Scaling to the next homonuclear diatomic, N_2 , involves putting two more electrons in the $2\sigma_g$ orbital, and the ordering of both the occupied and the unoccupied orbitals is preserved. In the case of these two molecules, the s/p interactions are significant enough to push the $2\sigma_g$ orbital above the π_u orbitals. This is not the case in the O_2 molecule in which the ordering of these orbitals is reversed. Scaling up to O_2 involves the addition of two more electrons, one of each placed in the two π_g orbitals for a ground state configuration of $(1\sigma_g)^2(1\sigma_u)^2(2\sigma_g)^2(\pi_u)^2(\pi_u)^2(\pi_g)^1(\pi_g)^1$. Since the molecular orbitals in our scaling scheme are based on the energetic ordering of the original carbon-carbon interaction, it cannot account for this switching of molecular orbitals. We do not believe that this discrepancy will notably impair our results as we are seeking a qualitative understanding of the dynamics of larger molecular systems.

Another limitation of this method is the failure to adequately differentiate between single and double bonds formed between carbon and oxygen molecules. Frauenheim and co-workers have attributed this difficulty to long range charge transfer effects and have included an adjustment to the charge distribution through a self-consistent field procedure [9]. We have chosen to adjust our calculations with a completely empirical procedure in which we scale the entire effective nuclear repulsion between carbon and oxygen atoms by a small constant that was determined by fitting to a group of simple organic test molecules. We have found that a value of 0.90 for a CO double bond and a value of 1.18 for a CO single bond gives reasonable results. We would like to point out that this scaling factor can be adjusted for specific molecules in order to improve accuracy.

Table 3 reports both the electronic and nuclear equilibrium properties of the diatomic molecules involved in the parameterization scheme. By scaling to the active

Table 3. Comparison of calculated and experimental bond lengths, vibrational frequencies, binding energies and excitation energies. In all cases, the experimental bond lengths and frequencies were taken from reference [10], the binding energies from reference [11], and the excitations energies from a B3LYP/aug-cc-pVQZ calculation, except for the bond lengths of NH and OH which were taken from reference [12], and the excitation energy of N₂ which was calculated with a non-augmented basis set.

Molecule	Property	Experimental	SERID
N ₂	r_o (Å)	1.0977	1.0982
	ω (cm ⁻¹)	2358.57	2352.54
	D_o (eV)	9.76	19.29
	ΔE_g (eV)	9.30	9.68
CN	r_o (Å)	1.1718	1.1724
	ω (cm ⁻¹)	2068.59	2062.18
	D_o (eV)	7.6	10.34
	ΔE_g (eV)	8.25	7.54
NH	r_o (Å)	1.0378	1.0403
	ω (cm ⁻¹)	3282.30	3240.56
	D_o (eV)	3.8	3.48
	ΔE_g (eV)	7.72	8.21
O ₂	r_o (Å)	1.2075	1.2082
	ω (cm ⁻¹)	1580.19	1576.93
	D_o (eV)	5.08	6.62
	ΔE_g (eV)	8.61	5.77
CO	r_o (Å)	1.1282	1.1287
	ω (cm ⁻¹)	2169.81	2163.61
	D_o (eV)	11.11	12.83
	ΔE_g (eV)	8.39	8.69
OH	r_o (Å)	0.9705	0.9724
	ω (cm ⁻¹)	3737.76	3705.94
	D_o (eV)	4.35	3.57
	ΔE_g (eV)	7.09	10.54
NO	r_o (Å)	1.1508	1.1515
	ω (cm ⁻¹)	1904.20	1897.28
	D_o (eV)	6.50	4.71
	ΔE_g (eV)	5.63	5.74

Table 4. Comparison of SERID calculated bond lengths to experimental bond lengths. Experimental values for pyrazine and pyrimidine taken from [13], values for pyridazine and pyridine taken from [14], values for tetrazine taken from [15], and values for triazine taken from [16].

Molecule	Bond	Exp. (Å)	SERID (Å)
Pyrazine	C–C	1.397	1.394
	C–N	1.338	1.359
	C–H	1.083	1.089
Pyridazine	N–N	1.337	1.336
	N–C _a	1.338	1.362
	C _a –C _b	1.400	1.393
	C _b –C _b	1.385	1.395
	C _a –H	1.079	1.092
	C _b –H	1.071	1.097
Pyridine	N–C _a	1.340	1.361
	C _a –C _b	1.395	1.396
	C _b –C _c	1.394	1.398
	C _a –H _a	1.084	1.090
	C _b –H _b	1.081	1.097
	C _c –H _c	1.077	1.097
Pyrimidine	C _a –N	1.328	1.353
	C _b –N	1.350	1.362
	C _b –C _c	1.393	1.392
	C _a –H _a	1.082	1.082
	C _b –H _b	1.079	1.090
	C _c –H _c	1.087	1.096
Tetrazine	C–N	1.341	1.359
	N–N	1.326	1.342
	C–H	1.073	1.082
Triazine	C–N	1.338	1.358
	C–H	1.084	1.084

space region, we can obtain very reasonable results for the HOMO–LUMO energy gap, ΔE_g . We also report very accurate bond lengths and vibrational frequencies as these were the values to which we scaled the effective nuclear repulsion. Unfortunately, this method sacrifices accuracy in the binding energy, D_o , of some of the diatomics. In order to obtain a smooth potential energy surface, we only fit to the vibrational frequencies and equilibrium bond lengths. We have applied this approach to a set of both nitrogen containing (see table 4) and oxygen containing (see table 5) molecules. In all cases, we obtain bond lengths that are usually within 2–3% of the experimental values and never in error by more than 5% of the experimental values.

3. Hydrogen–hydrogen interaction for small r

We mention that we have also re-parameterized the Frauenheim H–H data for small r in order to avoid convergence problems with respect to time step for excited

Table 5. Comparison of calculated and experimental bond lengths for various oxygen containing molecules. All experimental values are taken from [11], except for the values for acetic acid and ethanol which are taken from [10].

Molecule	Bond	SERID (Å)	Exp. (Å)
CO ₂	C–O	1.177	1.162
H ₂ O	O–H	0.979	0.957
Acetaldehyde	C _a –O	1.208	1.216
	C _a –C _b	1.520	1.501
	C _a –H	1.146	1.114
	C _b –H	1.097	1.086
	C–C	1.531	1.520
Acetic Acid	C–O _a	1.251	1.214
	C–O _b	1.361	1.364
	C–H	1.099	1.100
	O _b –H	0.965	0.971
	C _b –C _b	1.432	1.431
Furan	C _a –C _b	1.391	1.361
	C _a –O	1.363	1.362
	C–H	1.088	1.076
	C–C	1.534	1.515
Acetone	C–O	1.236	1.215
	C–H	1.097	1.086
	C _a –C _b	1.537	1.512
Ethanol	O–H	0.961	0.971
	C _a –O	1.415	1.431
	C _a –H	1.113	1.100
	C _b –H	1.096	1.090

state simulations. As can be seen in figure 1(a), the lowest unoccupied molecular orbital (LUMO) level tends to infinity for small internuclear separation in the H₂ molecule. In the small r region, the LUMO energy changes dramatically with a small change in bond length. This presents a convergence problem if the LUMO level has a finite population, i.e. if we are performing an excited state simulation. We believe the shape of the LUMO energy surface is due to the use of a minimal basis description. Figure 1(b), shows the highest occupied molecular orbital (HOMO) and LUMO energy levels calculated with the B3LYP functional and Dunning's aug-cc-pVQZ basis set. The LUMO level in this calculation remains fairly constant for small r . We have incorporated this effect into our parameters without altering either the large r results or the equilibrium (HOMO) values. In order to do this, we used the values of the original Frauenheim LUMO energies for values of r greater than or equal to 2.0 au, the B3LYP/aug-cc-pVQZ LUMO energies for values of r less than or equal to 1.8 au and a mixture of the two for r values between 1.8 and 2.0. The actual LUMO energy value for each value of r is obtained according to

$$\varepsilon_{\text{LUMO}}(r) = \varepsilon_{\text{LUMO}}^{\text{B3LYP}}(1.8) + \left(\varepsilon_{\text{LUMO}}^{\text{Original}}(2.0) - \varepsilon_{\text{LUMO}}^{\text{B3LYP}}(1.8) \right) \left(\frac{r - 1.8}{0.2} \right)^m.$$

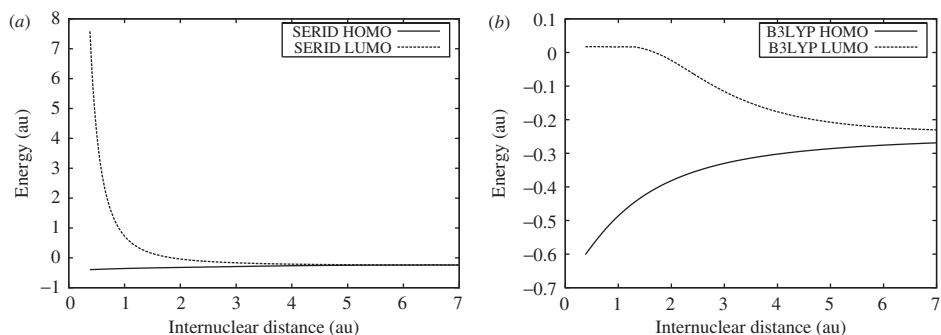


Figure 1. HOMO and LUMO energies calculated using (a) the original Frauenheim H and S matrix elements and (b) density functional theory with the B3LYP functional and the aug-cc-pVQZ basis set as a function of internuclear separation.

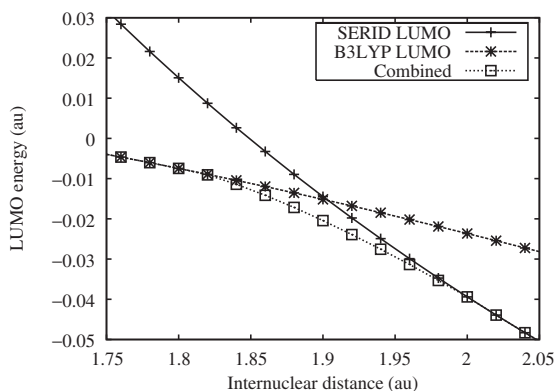


Figure 2. LUMO energy values for internuclear separation distances between 1.8 au and 2.0 au for the H_2 molecule calculated with the original Frauenheim parameters, B3LYP with the aug-cc-pVQZ basis set and an interpolation of the two.

We have found a value of m equal to 1.3 gives a reasonable fit (see figure 2). This scheme has the advantage that the coefficients for the effective nuclear repulsion do not have to be altered as we have left the HOMO energy unchanged. Once the HOMO and LUMO energies for each value of r are obtained it is simple to convert these to the H and S matrix elements utilized in the SERID simulations since the matrices for the H_2 molecule are 2×2 matrices in which $H_{12} = H_{21}$, $S_{12} = S_{21}$, $S_{ii} = 1.0$ and H_{ii} is the appropriately scaled atomic energy of hydrogen, E_d . The relations are:

$$S = \frac{2E_d - \varepsilon_{\text{HOMO}} - \varepsilon_{\text{LUMO}}}{(\varepsilon_{\text{HOMO}} - \varepsilon_{\text{LUMO}})},$$

$$H = \varepsilon_{\text{HOMO}}(1 + S) - E_d.$$

These expressions are only valid in the small r region where the energy difference between the HOMO and LUMO levels is finite. We have used these expressions to obtain values of H and S for r less than 2.0 au and kept the original Frauenheim values for r greater than 2.0 au.

4. DPA equilibrium properties

We have chosen to test our scaled nitrogen and oxygen parameters on the molecule dipicolinic acid (DPA or 2,6-pyridinedicarboxylic acid). This molecule is prevalent in bacterial spores [17, 18] and has been used as a marker molecule in various spectroscopic detection schemes [17, 19–22]. This molecule is an ideal test molecule for our parameters as it contains the atoms oxygen and nitrogen yet consists of a parent ring structurally similar to benzene, a molecule we have previously investigated with SERID [5, 23]. In order to explore the DPA molecule's response to a laser pulse, we first obtained an equilibrium geometry configuration and the corresponding ground state electronic properties. We equilibrated the molecule by running a 2000 fs simulation, without an applied laser pulse, in which the velocity of each atom was reduced by 0.3% at each time step. The initial temperature was set to 300 K and a time step of 10 as was used. As shown in figure 3, the energy of the molecule cooled down to a stable value of -799.67 eV. The equilibrium bond lengths resulting from this procedure are in agreement with those calculated by other *ab initio* methods (see table 6). The numbering and nomenclature for each atom in the molecule are described in figure 4. As also seen in other calculations [24, 25], SERID predicts DPA to have a planar geometry. The only notable difference between the SERID calculated geometry and geometries calculated by other methods is in the $H_aO_bC_d$ angle. SERID calculates this angle to be 86° whereas DFT and CASSCF predict it to be 107° [25] and 113° [24], respectively. We believe that this error in the SERID equilibrated geometry is due to the small cut-off value of the nuclear repulsion between hydrogen and carbon in the SERID parameters.

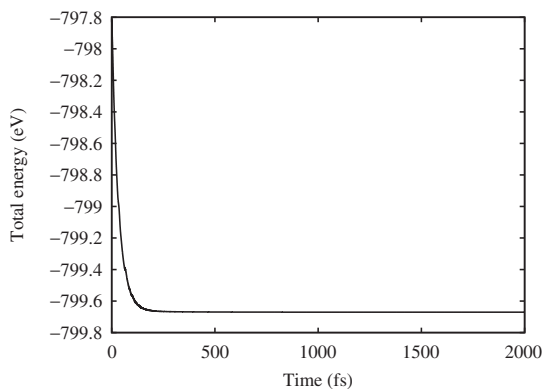


Figure 3. Convergence of the total energy of the molecule.

Table 6. Comparison of DPA equilibrium bond lengths between SERID calculation, a CASSCF calculation [24], a DFT calculation [25] and experiment [26].

Bond	SERID	MCSCF/6-21G	B3LYP/6-311 + G(2df, 2pdf)	Exp.
N-C _a	1.378	1.338	1.330	1.334
C _a -C _b	1.401	1.398	1.395	1.397
C _b -C _c	1.394	1.395	1.386	1.389
C _a -C _d	1.509	1.484	1.501	1.497
C _d -O _a	1.260	1.216	1.207	1.247
C _d -O _b	1.327	1.336	1.340	1.275
H _a -O _b	0.948	0.955	0.968	-
H _b -C _b	1.096	1.070	1.080	-
H _c -C _c	1.096	1.071	1.081	-

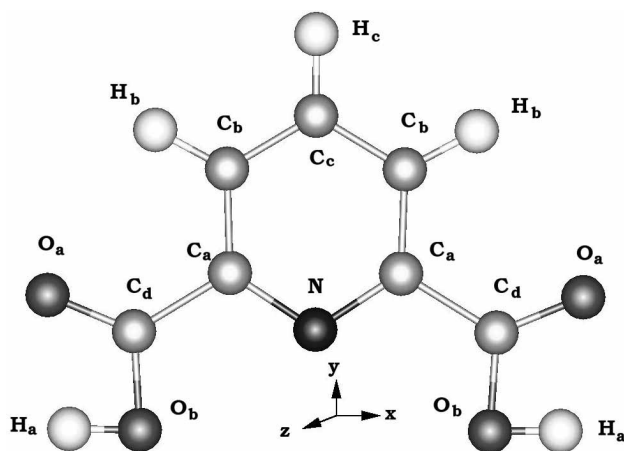


Figure 4. The nomenclature for each of the atoms in the equilibrated DPA molecule.

In our simulations, the hydrogen atom no longer ‘sees’ the carbon atom at 86° , resulting in a smaller bond angle. We believe this inconsistency to be minor for our present calculations.

The molecular orbital structure calculated by SERID is also in reasonable agreement with that calculated by DFT. In table 7, we compare the energy of the levels relevant to our calculations, the HOMO-3 through LUMO+1 levels with a B3LYP/6-311G + (2df, 2pd) calculation. These are the orbitals involved with the electronic transitions in our laser pulse simulations. In both cases, the three highest occupied molecular orbitals are nearly degenerate, spanning an energy difference of only 0.31 eV (SERID calculation). Similarly, both simulations also show that two lowest unoccupied energy levels are also nearly degenerate, with an energy difference of only 0.27 eV (SERID calculation). The energy gap between the HOMO and LUMO levels are also in qualitative agreement, 4.03 eV for the SERID calculation and 5.30 eV for the DFT calculation.

Table 7. Comparison of SERID and B3LYP/6-311 + G(2df, 2pd) HOMO-3 through LUMO+1 energy levels in DPA.

Level	SERID (eV)	B3LYP (eV)	SERID Symmetry	B3LYP Symmetry
HOMO-3	-7.79	-8.82	π (B_1)	π (B_1)
HOMO-2	-7.20	-8.19	π (A_2)	σ (B_2)
HOMO-1	-7.05	-8.09	n (A_1)	π (A_2)
HOMO	-6.89	-7.67	σ (B_2)	n (A_1)
LUMO	-2.86	-2.37	π (B_1)	π (A_2)
LUMO+1	-2.59	-2.24	π (A_2)	π (B_1)

Table 8. Comparison the vibrational frequencies calculated with SERID, CASSCF [24], DFT [25] and experiment [27].

Description	SERID (cm^{-1})	CASSCF (cm^{-1})	DFT (cm^{-1})	Exp. (cm^{-1})
Ring bend	702	697	644	647
Ring breath	1070	1086	1015	987
Ring breath/OH bend	1270	1338	1231	1275
Ring stretch	1671	1723	1614	1571
Ring stretch	1738	1742	1619	1576

We have also calculated several of the normal modes of DPA. The modes shown in table 8 are the modes that are primarily excited during our laser pulse simulations. These modes were obtained by assigning an initial velocity to each atom that mimicked the normal coordinates of the desired mode. The simulation was allowed to run for 1000 fs at 300 K with a time step of 10 as. The velocity autocorrelation function was then Fourier transformed in order to obtain the spectrum. Due to the finite run time of our simulations, each reported normal mode value calculated by the SERID method has an uncertainty of $\pm 33 \text{ cm}^{-1}$.

5. First excited state of DPA

In order to determine the nature of the first excited state transition of DPA, we subjected the equilibrated molecule to a 5 fs FWHM laser pulse with a frequency matched to the HOMO-LUMO gap energy of the molecule, 4.03 eV. We ran two simulations, one with a polarization in the x direction and one with a polarization in the y direction (coordinate system described in figure 4). The total duration of both simulations was 1010 fs with a time step of 1 as. The temperature was set to zero in order to analyse the motion of the nuclear solely due to interactions with the laser pulse. Neither polarization exhibited a significant excitation out of the occupied n or σ orbitals. The x -polarized light induced a significant π (A_2) to π^* (B_1) excitation and the y -polarized light induced a significant π (A_2) to π^* (A_2) excitation (figure 5).

We then compared these excitations to a TDDFT calculation performed with the B3LYP hybrid functional and the 6-311 + G(2df, 2pd) basis set [25]. The first four

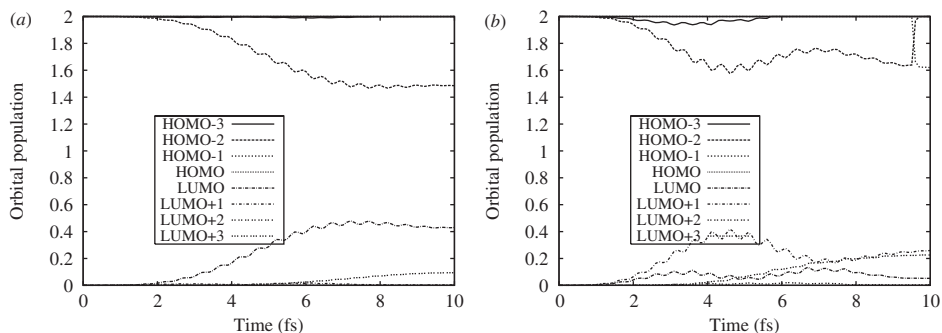


Figure 5. HOMO-3 through LUMO+3 level occupation for a DPA molecule subjected to a 5 fs (FWHM) laser pulse with a frequency of 4.03 eV and (a) a fluence of 0.022 kJ m⁻² polarized in the *x* direction and (b) a fluence of 0.105 kJ m⁻² polarized in the *y* direction.

excited states involve transitions from the *n* and σ occupied molecular orbitals into either of the two π low lying unoccupied orbitals. In each case, the transition is either dipole forbidden or has an extremely small oscillator strength with the exception of the second excited state. This transition has a small oscillator strength, 0.0013, and consists of a transition from an *n* orbital to a π (B_1) transition. This transition does not appear in the SERID simulations. Since we used a very short pulse (5 fs FWHM) in these simulations, this weak transition is overshadowed by more dominant transitions occurring at higher energies. The first TDDFT calculated excited state transition with a significant oscillator strength, occurs at an excited state energy of 5.05 eV. This transition involves excitations from the π (B_1) level to the π^* (A_2) level and from the π (A_2) to the π^* (B_1) level. The electric dipole moment lies completely in the *x* direction. The second transition with an appreciable oscillator strength occurs with an excitation energy of 5.37 eV and involves a transition from the π (B_1) level to the π^* (B_1) level and from the π (A_2) to the π^* (A_2) level. The dipole moment lies completely in the *y* direction. Although there are slight differences in the ordering of the molecular orbitals between the two methods, the nature of the transition is the same. The SERID simulations show qualitative agreement with the TDDFT calculations.

6. Summary

We have presented a simple scheme that scales carbon and hydrogen pairwise interactions to include nitrogen and oxygen within the framework of a tight-binding semi-empirical calculation. The scheme involves scaling the Hamiltonian matrix to fit the new electronic properties and scaling the effective nuclear repulsion to fit the new nuclear properties. We have used the parameters to obtain equilibrium bond lengths for a variety of nitrogen and oxygen containing test molecules. In all cases the bond lengths are within 5% of the experimental values. As a more in depth case study we have simulated both the equilibrium and excited states of DPA. These results were

shown to be in qualitative agreement with other fully *ab initio* methods. We used the Gaussian03 package for all of the density functional theory calculations presented in this work [28].

Acknowledgments

This work was supported by the Robert A. Welch Foundation, Grant A-0929.

References

- [1] A good review can be found in A. Zewail, *Pure Appl. Chem.* **72** 2219 (2000).
- [2] Y. Dou, B.R. Torralva and R.E. Allen, *J. Mod. Opt.* **50** 2615 (2003).
- [3] D. Porezag, Th. Frauenheim, Th. Koehler, *et al.*, *Phys. Rev. B* **51** 12947 (1995).
- [4] Y. Dou and R.E. Allen, *J. Mod. Opt.* **51** 2485 (2004).
- [5] B.R. Torralva and R.E. Allen, *J. Mod. Opt.* **49** 593 (2002).
- [6] B.R. Torralva, T.A. Niehaus, M. Elstner, *et al.*, *Phys. Rev. B* **64** 153105 (2001).
- [7] J.B. Mann, LA-3690 (Los Alamos National Laboratory, USA, 1967)
- [8] T.H. Dunning, *J. Chem. Phys.* **90** 1007 (1989).
- [9] M. Elstner, D. Porezag, G. Jungnickel, *et al.*, *Phys. Rev. B* **58** 7260 (1998).
- [10] *CRC Handbook of Chemistry and Physics*, 85th ed. (CRC Press LLC, New York, 2004) (online edition).
- [11] G. Herzberg, *Molecular Spectra and Molecular Structure I. Spectra of Diatomic Molecules*, 2nd ed. (Krieger Publishing Company, Florida, 1989).
- [12] H. Sun, M.G. Sheppard and K.F. Freed, *J. Chem. Phys.* **74** 6842 (1981).
- [13] S. Craddock, P.B. Liescheski, D.W.H. Rankin, *et al.*, *J. Am. Chem. Soc.* **110** 2758 (1988).
- [14] C. Hannay, D. Dufлот, J.-P. Flament, *et al.*, *J. Chem. Phys.* **110** 5600 (1999), and references therein.
- [15] C. Haettig, O. Christiansen, S. Coriani, *et al.*, *J. Chem. Phys.* **109** 9237 (1998), and references therein.
- [16] Y. Osamura, M. Unno and K. Hashimoto, *J. Am. Chem. Soc.* **109** 1370 (1987), and references therein.
- [17] E. Ghiamati, R. Manoharan, W.H. Nelson, *et al.*, *Appl. Spectrosc.* **46** 357 (1992).
- [18] W.H. Woodruff, T.G. Spiro and C. Gilvarg, *Biochem. Biophys. Res. Commun.* **58** 197 (1974).
- [19] A. Alimova, A. Katz, H.E. Savage, *et al.*, *Appl. Opt.* **42** 4080 (2003).
- [20] S. Sarasanandarajah, J. Kunthandnil, B.V. Bronk, *et al.*, *Appl. Opt.* **44** 1182 (2005).
- [21] D. Pestov, M. Zhi, Z. Sariyanni, *et al.*, *PNAS* **102** 14976 (2005).
- [22] M.O. Scully, G.W. Kattawar, R.P. Lucht, *et al.*, *PNAS* **99** 10994 (2002).
- [23] P. Sauer, R.H. Xie, Y. Dou, *et al.*, *J. Mod. Opt.* **52** 2423 (2005).
- [24] H.F. Hameka, J.O. Jensen, J.L. Jenson, *et al.*, *J. Mol. Struct. (Theochem)* **365** 131 (1996).
- [25] J.R. Xie, V.H. Smith and R.E. Allen, *Chem. Phys.* **322** 254 (2006).
- [26] V.C. Téllez, B.S. Gaytán, S. Bernés, *et al.*, *Acta. Cryst.* **C58** o228 (2002).
- [27] P. Carmona, *Spectrochim. Acta* **36** 707 (1979).
- [28] M.J. Frisch, G.W. Trucks, H.B. Schlegel, *et al.*, Gaussian03, Revision C.02 (Gaussian, Inc., Wallingford CT, 2004).